

# Quartz crystal microbalance in elevated temperature viscous liquids: Temperature effect compensation and lubricant degradation monitoring

Dianxia Wang<sup>a</sup>, Paria Mousavi<sup>b</sup>, Peter J. Hauser<sup>b</sup>,  
William Oxenham<sup>c</sup>, Christine S. Grant<sup>a,\*</sup>

<sup>a</sup> Department of Chemical & Biomolecular Engineering, North Carolina State University, Raleigh, NC 27695-7905, USA

<sup>b</sup> Department of Textile Engineering, Chemistry & Science, North Carolina State University, Raleigh, NC 27695-8301, USA

<sup>c</sup> Department of Textile & Apparel Technology & Management, North Carolina State University, Raleigh, NC 27695-8301, USA

Received 21 May 2004; received in revised form 20 April 2005; accepted 5 May 2005

Available online 9 September 2005

## Abstract

The quartz crystal microbalance (QCM) was extended to investigate viscous liquids at elevated temperatures in both isothermal and non-isothermal systems. An analysis of the frequency–temperature behavior of the QCM resulted in a new approach to compensate for the effect of the rate of temperature rise on the theoretical QCM temperature coefficients. The temperature-dependent viscosities of a series of liquids were evaluated by measuring the damping voltage of QCM. Thermal degradation experiments on pentaerythritol tetrapelargonate based lubricants demonstrated the potential application of QCM as an in situ sensor to evaluate the thermal stability of lubricants or other viscous fluids. The solid residue deposition rates and liquid phase property changes (i.e., product of density and viscosity) were extensively investigated by monitoring variations in the QCM frequency and damping voltage during the lubricant thermally stressing over a temperature range of 150–220 °C.

© 2005 Elsevier B.V. All rights reserved.

**Keywords:** Quartz crystal microbalance; Viscosity; Deposition; Lubricant; Thermal degradation

## 1. Introduction

The quartz crystal microbalance (QCM), as an in situ sensor, has played important roles in probing interfacial processes both at surfaces and in thin films. The high mass sensitivity, conceptual simplicity, miniature size, high tolerance to extreme environments and low cost of the QCM portend its development in a diverse variety of commercial and research applications [1,2]. The QCM was first introduced for use in a vacuum system for deposition measurements by Sauerbrey in the late 1950s [3]. In 1982, Nomura and Okuhara showed that the QCM can be made to oscillate in a liquid [4]. After that, increased attention was placed on the application of the QCM for the study of solid–liquid interfaces [1,2]. When a QCM sensor contacts a liquid, the frequency shift

has contributions from both rigid mass accumulation and liquid property changes, while the motional resistance increase is generated only from liquid property changes [5,6]. The simultaneous measurement of frequency shift and motional resistance changes during QCM operation with viscoelastic films allows a separation of frequency contributions due to liquid property changes and mass changes on the electrode surface.

Pressure, temperature and roughness of the electrode surface as well as mass load and viscous damping affect the resonant frequency of the quartz crystal [7,8]. When a polished crystal is used in liquid under ambient pressure conditions, the effects of pressure and roughness can be neglected. However, even though the commonly used AT-cut crystals have lower temperature coefficients in the vicinity of room temperature, the resonant frequency of the crystal becomes extremely sensitive to temperature change at elevated temperatures. Unfortunately, a temperature shift is unavoidable

\* Corresponding author. Tel.: +1 919 515 2317; fax: +1 919 515 3465.  
E-mail address: grant@eos.ncsu.edu (C.S. Grant).

in a number of physical and chemical processes. Examples of potential temperature variations include: (1) processes resulting in a temperature shift due to chemical reactions or other heat generating events; (2) a required gradient temperature change in the process (e.g., heating or cooling down periods); (3) systems in which the temperature is difficult to control at a constant value.

Recent technological advances in textiles, jet aircraft and engine industries have placed an ever increasing heat load on functional organic chemicals such as lubricants, coolants and other kinds of processing aids [9–11]. Exposure of these chemicals to high temperatures results in the formation of solid residues, often called vanish/char/coke, on hot solid surfaces. The buildup of insolubles is of great concern because of the resulting possibility of systems failure and subsequent economic losses. A great deal of research has been conducted to evaluate the solid residual deposition characteristics when the chemicals thermally degrade. However, previous experimental tests were generally conducted under accelerated test conditions due to the lack of a sensitive tool for in situ evaluation of small amounts of deposits that occur when materials are thermally stressed. The major problem with accelerated testing is that the temperature/oxygen concentration values exceed the amounts expected during actual process conditions. In addition, the mass deposition rate is commonly determined after the test, resulting in only an estimated average deposition rate over the test duration. The increasing need for improving thermal stability of processing chemicals has promoted a strong requirement of a quantitative, in situ measurement method to investigate solid residuals deposition on metal surfaces.

This paper presents: (1) a modeling method for the compensation of temperature effects in the QCM measurements at elevated temperatures; (2) a methodology to use the QCM as an elevated temperature viscometer; (3) an approach to in situ monitoring both mass deposition rates and property changes of viscous liquids using the QCM at elevated temperatures. Studies are conducted under conditions of an increasing-temperature scenario and at isothermal conditions. A pentaerythritol tetrapelargonate based lubricant was employed as a sample liquid to demonstrate the utilization of QCM as an in situ sensor to monitor the mass deposition rate and property changes of viscous liquids.

## 2. QCM approach in viscous liquid at elevated temperatures

### 2.1. Basic principles

The QCM is comprised of a thin quartz crystal sandwiched between two metal electrodes that establish an alternating electric field across the crystal, causing vibrational motion of the crystal at its resonant frequency. This resonant frequency is sensitive to mass changes on the electrode surface, and is also affected by: (1) the properties (i.e., density and

viscosity) of the fluid in contact with the crystal and (2) the temperature and pressure of the crystal environment [12]. The roughness of the electrode surface and the mechanical stresses are also reported as parameters contributing to the resonant frequency shift [7]. However, in most thin-film deposition processes, the stress effect is small and its contribution can be neglected. The frequency shift caused by the roughness effect can be neglected also when polished crystals are used. In addition, the pressure (that means the hydrostatic pressure) in most liquid systems can be maintained at a constant value by always keeping the crystal immersed in a liquid at a constant depth [13]. In most cases, one is more interested in the frequency change, rather than the absolute frequency value. Consequently, the measured frequency shift can be written as:

$$\Delta F = \Delta F_m + \Delta F_\eta + \Delta F_T \quad (1)$$

where  $\Delta F$  is the frequency change, the subscripts  $m$ ,  $T$  and  $\eta$  refer to the pure mass, temperature and viscosity effects, respectively.

The well known Sauerbrey equation presents the relationship between the mass load and the associated frequency shift as [3]:

$$\Delta F_m = \frac{-2nF_0^2 \Delta m}{(\mu_q \rho_q)^{1/2}} \quad (2)$$

where  $\Delta m$  is the loaded mass per surface area,  $F_0$  the unperturbed resonant frequency,  $\mu_q = 2.947 \times 10^{11} \text{ g}/(\text{cm s}^2)$  and  $\rho_q = 2.648 \text{ g}/\text{cm}^3$  are the quartz shear stiffness and mass density, respectively, and  $n$  is the number of sides of the crystal in contact with the liquid. To obtain the amount of loaded mass with Eq. (2), the critical issue is to find out the contributions due to the temperature effect and the viscous damping indicated in Eq. (1).

### 2.2. Viscous damping

The viscous-effect,  $\Delta F_\eta$ , describes the interaction of the vibrating crystal with a viscous medium. This interaction leads to a decrease in frequency. For a Newtonian fluid, a mathematical expression was derived by Kanazawa and Gordon [14] to describe the relationship between the viscosity–density product and the associated frequency shift as:

$$\Delta F_\eta = -nF_0^{3/2} \left( \frac{\rho\eta}{\pi\mu_q\rho_q} \right)^{1/2} \quad (3)$$

where  $\rho$  and  $\eta$  refers to the density and viscosity of the fluid in which the crystal is immersed. The fluid properties, especially the viscosity, may change due to: (1) variations in temperature, (2) changes in concentration of the solution and (3) polymerization of the organic liquid during thermal degradation. It is clear that the measurement of the resonant frequency alone cannot distinguish changes in mass load from changes in liquid properties.

On the other hand, upon liquid loading, energy losses arise from the propagation of the standing acoustic wave into the liquid. For a completely wetted system, the power dissipation is predominated by the bulk properties of the liquid [15]. Muramatsu [5] showed that for a QCM in contact with liquid, the motional resistance is proportional to the square root of the liquid viscosity–density product. Martin et al. [6] have derived an analytical expression from which the resulting motional resistance is simply as follows:

$$R = R_0 + b(\rho\eta)^{1/2} \quad (4)$$

where  $R$  is the motional resistance,  $R_0$  presents the motional resistance for unperturbed QCM, while the second item relates to the motional resistance due to liquid loading.  $R_0$  and the constant  $b$  can be calculated from the properties of the quartz crystal [6]. An increase of the density–viscosity product of the liquid results in an increase in energy dissipation and thus a proportional increase in  $R$ . As a result, the measurement of the motional resistance enables the calculation of the value of  $(\rho\eta)^{1/2}$  (Eq. (4)). Further analysis enables one to obtain the frequency shift attributable to the liquid loading (Eq. (3)). In addition, if the density of the fluid does not change significantly, the QCM can be used as an in situ viscometer.

### 2.3. Compensation for temperature effect

The absolute temperature limit for the QCM measurements is the Curie point of quartz (573 °C), the point at which the piezoelectric properties disappear [16]. The temperature coefficients of crystals are critical functions of the angle of the crystal cut. For AT-cut crystals, this temperature coefficient is very low around room temperatures. For example, a frequency change of about 1 ppm/°C was observed in the temperature range from 10 to 50 °C. However, the frequency is very sensitive to temperature variations at high temperatures. Hence, the precision of the mass measurement is reduced at elevated temperatures.

There are basically two different approaches utilized to compensate for the aforementioned temperature effect: (1) using two QCM crystals, a reference crystal and a sensing crystal and (2) modeling. In the first approach, the reference crystal is protected so that no mass loading or liquid damping occurs and therefore only temperature changes affect the observed frequency. When the reference crystal frequency is subtracted from the sensing crystal frequency, the temperature effect is removed. The second approach is based on the idea that the drift of the QCM frequency baseline caused by the temperature effect follows a function that can be modeled.

In order to effectively eliminate the temperature effect by using a reference crystal, the sensing and reference crystals should fulfill the following conditions: (1) both crystals should be identical or very close in the basic frequency, electrode area and temperature coefficient and (2) the thermal environment of the reference crystal must be identical to that

of the sensing crystal, particularly with regard to the system thermal gradients. Although it is argued that using the reference crystal is the best way to compensate for the temperature effect [17], the following disadvantages limit the application of the reference crystal: (1) the difficulty to find two crystals that are identical; (2) the change in temperature of the covered reference crystal is somewhat delayed compared to the temperature change of the sensing crystal; (3) the reference crystal is difficult to cover accurately to avoid the gas diffusion onto the reference crystal surfaces; (4) using the reference crystal requires additional QCM cell volume and requires a more complicated electronic system. On the other hand, some of these problems can be avoided.

The frequency–temperature characteristics of an AT-cut crystal are usually described by a power series of the third order in the temperature [18]:

$$\Delta F_T = a_3T^3 + a_2T^2 + a_1T + a_0 \quad (5)$$

where  $T$  is the temperature (°C),  $a_0$ – $a_3$  are the temperature coefficients, which are reported to be dependent on angles of cut, ratio of crystal dimensions, order of overtone, shape of plate and type of mounting [19]. The current research indicates that these coefficients are not only functions of aforementioned parameters but are also affected by the rate of temperature change. The latter effect is critical to accurately utilize the modeling compensation method, since the coefficients are obtained from independent tests where temperature changes may not occur at the same rate as actual mass accumulation experiments. The dependence of  $a_0$ – $a_3$  on the rate of temperature change will be discussed extensively in Section 4.1.

## 3. Experimental

### 3.1. Materials

Compressed helium (HP grade, 99.997%), nitrogen (UHP grade, 99.999%) and air were purchased from National Welders and used as received. Organic solvents of HPLC grade ethanol, acetone, tetrahydrofuran, tridecane, hexadecane and heptadecane, were obtained from Sigma–Aldrich. Commercial grade pentaerythritol tetrapelargonate based lubricant, designated as EM, was obtained from Cognis and used without any further purification.

### 3.2. QCM apparatus and crystals

The crystals utilized are 5 MHz AT-cut wafers with polished gold electrodes on both sides. All crystals are purchased from International Crystal Manufacturing (ICM). The crystal dimensions are: 1.36 cm blank diameter and 0.66 cm electrode diameter. The quartz crystal is driven by a Lever Oscillator (ICM). The Lever Oscillator is specially designed for QCMs operating in a viscous liquid and has been successfully

utilized in previous work [20]. The oscillator has two outputs: (1) a frequency output measured by an Agilent 225 MHz Universal Frequency Counter (model 5313A) and (2) a dc voltage signal, proportional to motional resistance,  $R$ , measured by a digital multimeter (model 34401A, Agilent Technologies). The time-dependent frequency and voltage readings are written to a computer by means of Agilent Ituilink Connectivity software.

### 3.3. Experimental methods

#### 3.3.1. Temperature dependence of the QCM response

The temperature dependence of the QCM frequency was measured in a helium environment. Each quartz crystal was cyclic thermally treated (three cycles in a temperature range of 35–250 °C) and cleaned prior to use in the following order: washing with deionized water, 0.4% sulfuric acid solution, deionized water and ethanol; followed by drying with flowing nitrogen gas; in the final step the crystal was cleaned with an ultraviolet/ozone cleaner (Jelight Co. Model 42, Suprasil lamp). The clean crystal was placed in a small stainless steel cell (dimensions 1.9 cm × 1.8 cm × 0.8 cm). A thermocouple probe was welded on the crystal holder and mounted into the cell to monitor the temperature change inside the cell. Helium flowed through the cell at a very slow rate (2.0 ml/min). The cell was put into a gas chromatography oven to either maintain a constant temperature or to obtain a constant rate of temperature rise. The values of the QCM frequency and temperature were continuously recorded (every second) while the oven was heated from 35 to 250 °C.

Two types of frequency–temperature behavior tests were carried out, namely, a stepwise-increase test and a continuous-increase test. In the first case, the temperature was increased stepwise, that means keeping temperature at each desired value until the steady value of frequency fluctuation (less than ±1 Hz) was observed for 10 min. During the continuous-increase tests, the temperature was increased continuously at constant rates of 5, 10, 15 and 20 °C/min. The first group of tests was conducted to ascertain the absolute temperature dependence of the QCM frequency. The latter tests were done to investigate the delay in the response of the QCM to temperature change. Duplicate experiments for each test condition were conducted to obtain average frequency data.

#### 3.3.2. Viscosity measurements with QCM

The viscosity measurements with QCM for a series of organic solvents were carried out in a custom-made thermal cell (Fig. 1). The thermal cell was a 215 ml stainless steel vessel (6 cm i.d. and 7.6 cm high) with a thick stainless steel lid. A custom-built QCM electrical feedthrough, gas phase inlet and outlet ports, and two thermocouple probes (one is immersed in the liquid phase and the second is suspended in the gas phase) are mounted in through the lid. The crystal was suspended vertically in the liquid in order to

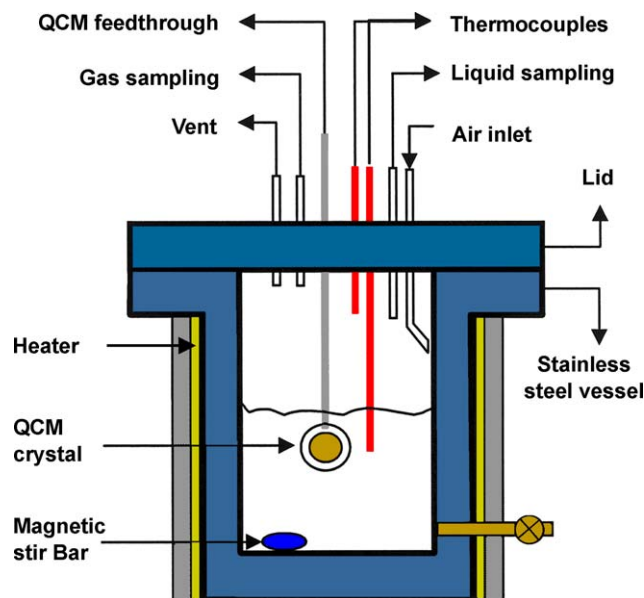


Fig. 1. Schematic of thermal cell.

minimize gravitational effects. The thermal cell was heated with a custom-made heater regulated by a temperature controller via a thermocouple immersed in the liquid. A magnetic stirrer was used to minimize spatial temperature gradients. The liquid phase thermocouple probe and the QCM sensor were installed in positions the same distance to the wall of the cell. In addition, the QCM sensor and the thermocouple probe were placed very close (2 mm). Hence, the temperature monitored by the thermocouple probe is considered the same as that of the QCM sensor. The liquid temperature inside the thermal cell was maintained at ±0.1 °C over a temperature range from room temperature (approximate 25 °C) to 300 °C.

In a typical measurement, the cell was filled with 100 ml of liquid and heated to a specific temperature, the values of the dc voltage signals were continuously recorded (every 5 min) until steady state (fluctuation of dc voltage value less than ±0.001 V) was maintained for 10 min. The temperature set point was then increased to a new value to obtain a new stabilized voltage value.

Three sets of measurements were conducted on the voltage values for different organic liquids over a range of temperatures: (1) tridecane, hexadecane and heptadecane over a temperature range of 50–300 °C; (2) ethanol, acetone and tetrahydrofuran at 20 °C; (3) lubricant EM over a range of 150–220 °C. The measured voltage values of ethanol, acetone, tetrahydrofuran, tridecane and hexadecane were used to generate a calibration curve for the relationship between  $(\rho\eta)^{1/2}$  and the voltage value. The liquid property values of these pure chemicals are available at specific temperatures from a handbook [21]. The viscosities of heptadecane and the lubricant EM were obtained from a calculation using the calibration curve generated in this work.

### 3.3.3. Lubricant degradation

In the lubricant degradation experiments, the thermal cell was filled with 136 ml of lubricant. The QCM crystal and cell had the same configuration as mentioned above for the viscosity tests. Pre-heated dry air was continuously fed into the cell at a constant flow rate of 21.0 ml/min. The lubricant was continuously heated from the room temperature to a set point of 220 °C and was maintained at  $220 \pm 0.1$  °C for 10 h. The resonant frequency, the dc voltage signal and the temperature of the lubricant were recorded at 5 s intervals.

## 4. Results and discussion

### 4.1. Frequency–temperature characteristics

The frequency–temperature characteristics of an AT-cut quartz resonator operating in the temperature range from –60 to 80 °C are usually described by a power series of the third order in the temperature [12,18,22,23]. Bechmann indicated that the third order expression for the frequency–temperature characteristics satisfactorily describes the behavior of an AT-cut quartz resonator within the limits of –200 to 250 °C; beyond this range higher order terms must be considered [22]. It is found in the current research that the frequency–temperature data cannot be correlated utilizing the same cubic function in both the elevated temperature range (e.g., 100–260 °C) and in the lower temperature range (e.g., 20–100 °C). Fig. 2 shows the temperature-dependent frequency shift measured during the stepwise-increase-temperature tests described in Section 3.3.1. The least-squares best-fitted equations for the experimental results in the different temperature ranges are listed below.

In the lower temperature range:

$$\Delta F_T = 0.000468T^3 - 0.0306T^2 + 0.84T + 47.7 \quad (6)$$

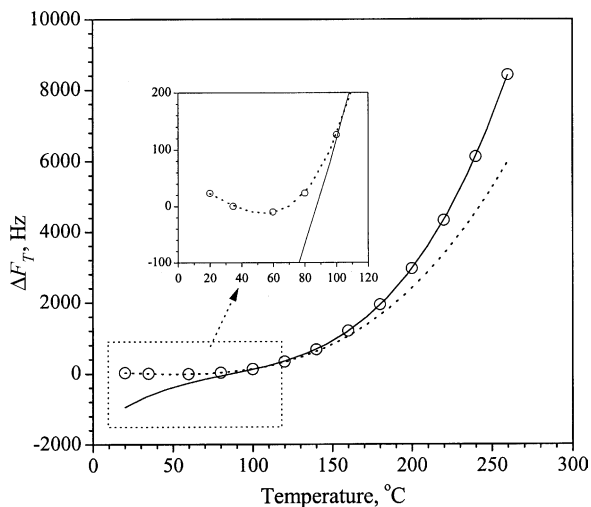


Fig. 2. Plots of frequency shift vs. temperature measured from the stepwise-increase-temperature tests (in air). Open circles represent experimental values, solid and dot lines represent Eqs. (6) and (7), respectively.

In the elevated temperature range:

$$\Delta F_T = 0.001281T^3 - 0.3262T^2 + 36.52T + 1555.7 \quad (7)$$

The temperature coefficients provided in Eq. (6) are very close to the values reported in the literature [12,18,22,23]. However, no literature data has been found in extended temperature ranges. The shift of temperature coefficients ( $a_0$ – $a_3$ ) observed around 100–120 °C can be attributed to the change of quartz thermal properties (e.g., expansion coefficient) occurring over this temperature range [24].

As mentioned above, the data shown in Fig. 2 were obtained from the stepwise-increase tests, i.e., the rate of temperature increase ( $r$ ) equals zero when the steady value of frequency was measured at each specific temperature set point. Therefore, the coefficients derived in Eqs. (6) and (7) express the sole effect of temperature on the QCM frequency. However, it was observed in the current research that the temperature coefficients,  $a_0$ – $a_3$  (see Eq. (5)), are also functions of the rate of temperature increase in the case of a continuous temperature increase. Fig. 3 shows the frequency change with temperature when the temperature increases at varying rates over the elevated temperature range. The observed frequency shift becomes smaller with the increase in the rate of temperature rise; the reduction is more pronounced at higher temperature. This observation indicates that there is a time delay in the QCM frequency response associated with the temperature change.

The variation of the temperature coefficients ( $a_0$ – $a_3$ ), obtained from correlating the frequency–temperature data (Fig. 3) over a temperature range of 140–220 °C, with the rate of temperature increase is presented in Fig. 4. In the tested rate range of 0–20 °C/min, the temperature coefficients can be correlated to the rates with the third polynomial relations with good correlation coefficient values (see Fig. 4). During high temperature lubricant thermal degradation, the

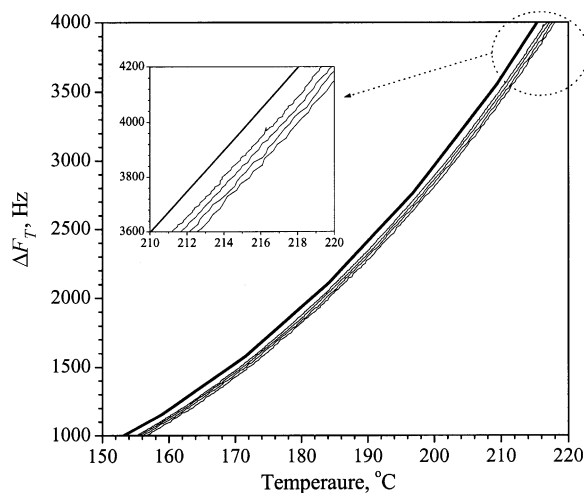


Fig. 3. Frequency shift vs. temperature measured from the continuous-increase-temperature tests. The rates of temperature increase associated with the lines shown from left to right: 0, (stepwise-increase-temperature tests), 5, 10 15 and 20 °C/min.

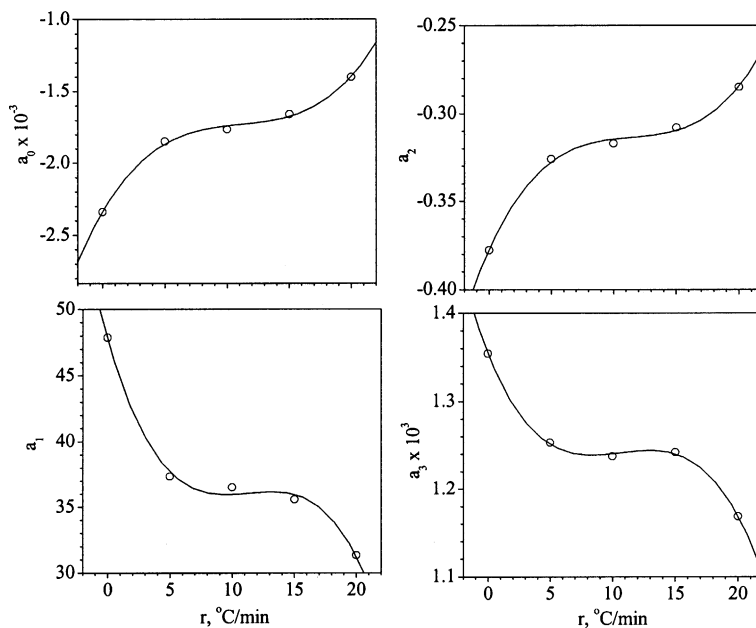


Fig. 4. Correlation of temperature coefficients with rates of temperature increase (temperature range: 140–220 °C). Open circles represent values obtained from Fig. 3; solid lines represent least-square best-fitted correlation equations listed below. Least-squares best-fitted correlation equations:  $a_0 = 0.3712r^3 - 12.415r^2 + 146.74r - 2336.2$ ;  $a_1 = (-0.8677r^3 + 29.582r^2 - 327.18r + 4775.5) \times 10^{-2}$ ;  $a_2 = (0.3774r^3 - 12.954r^2 + 154.43r - 3772.7) \times 10^{-4}$ ;  $a_3 = (-0.1090r^3 + 3.487r^2 - 35.40r + 1354.6) \times 10^{-6}$ .

forementioned correlations are used to calculate the temperature coefficients,  $a_0$ – $a_3$ , associated with the varying rates of temperature increase. This enables a determination of the frequency shift due to the temperature effect. This work focuses on the frequency–temperature behavior in the elevated temperature range corresponding to the lubricant degradation experiments. In addition, no related previous research incorporates the frequency–temperature behavior with the rate of temperature increase.

#### 4.2. In situ measurement of temperature dependence of viscosity

The determination of in situ viscosity values is important to a variety of physical/chemical processes. This is especially true during investigations of the thermal degradation of lubricants, jet fuels and other chemical processing aids. In these applications, the real time viscosity values at elevated temperatures are needed to accomplish the predictive modeling of degradation mechanisms [25]. In addition, real time viscosity values are essential in calculating the mass accumulation when the QCM is used to monitor the adsorption, desorption and deposition processes (see Eqs. (1) and (3)).

According to the design of the Lever oscillator utilized in this research [20], the damping voltage ( $V$ ) is proportional to the motional resistance  $R$ . Hence, the value of  $V$  should correlate to the square root of viscosity–density product of the liquid in a linear relationship (see Eq. (4)). To measure the viscosity using the QCM, the damping voltage values were determined for various organic liquids for which the viscosities and densities are available from the literature.

The responses of damping voltage to various liquid loadings are shown in Fig. 5. The solid line represents the following least-squares fit equation for the damping voltage and viscosity–density product data:

$$V = 1.3951 + 3.8611(\rho\eta)^{1/2} \quad (8)$$

Theoretically, the intercept value 1.3951 (defined as  $V_1$  here) should reflect the motional resistance,  $R_0$ , for an unperturbed QCM (Eq. (4)). The  $R_0$  can be calculated from an equation derived by Martin et al. [6]. The value obtained is 0.44  $\Omega$  for a 5 MHz QCM in a fundamental mode. This value

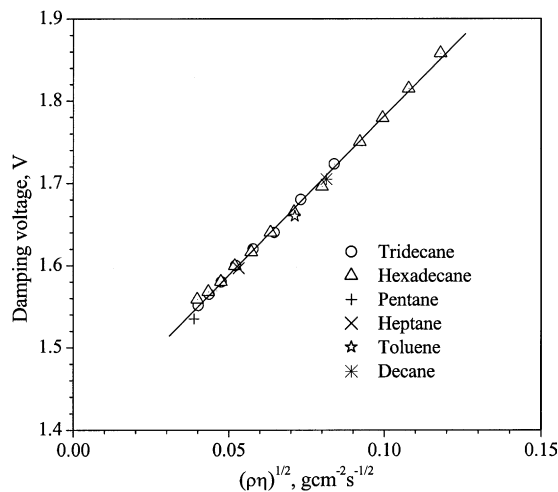


Fig. 5. Plot of measured damping voltage vs. square root of viscosity–density product of listed chemicals in the temperature range of 20–300 °C. Solid line represents least-squares best-fitted linear correlation.

is negligibly small when compared with the total motional resistance  $R$  for a QCM immersed into a liquid. However, the practical measured value of the motional resistance for an unperturbed QCM (defined as  $R_1$  here, and its value is  $55.3 \Omega$  based on Martin's work) is significantly greater than the calculated value of  $R_0$ . This indicates the presence of energy losses other than the viscous damping, such as the losses in the electrodes and in the crystal sensor mounting [6]. It is apparent that the intercept obtained in above correlation is significant; it is a value that cannot be neglected. This observation is in agreement with the previous work by Martin et al., and Yang and Thompson [6,15]. Due to the loss caused by the crystal sensor mounting, the individual operating difference might induce the variation in  $V_1$ , further introducing an error in the viscosity measurement. To correct  $V_1$ , the damping voltage of the crystal in air was measured for the crystal mounting in the present research:

$$V_{\text{air}} = V_1 + 3.8611[(\rho\eta)^{1/2}]_{\text{air}} \quad (9)$$

Combining the density–viscosity product of air at the specific temperature, Eq. (8) can be rewritten utilizing the expression for the modified  $V_1$  for our mounting configuration:

$$V = \{V_{\text{air}} - 3.8611[(\rho\eta)^{1/2}]_{\text{air}}\} + 3.8611(\rho\eta)^{1/2} \quad (10)$$

A comparison between the QCM derived viscosity values of heptadecane over a temperature range of 60–300 °C and those from literature [21] indicates a good agreement (Fig. 6a). Fig. 6b shows the temperature dependent viscosity for the polyol ester lubricant EM determined using the QCM.

#### 4.3. Deposition kinetics of thermally stressed lubricant

Previous investigations have proposed mechanisms related to oil (ester lubricants, mineral oils, fuels, etc.) thermal degradation in the presence of oxygen [9,10,26]. It is generally agreed that the primary oxidation products formed in the system undergo further polymerization producing high molecular weight oxy-polymeric compounds that form deposits. The QCM in the present work was used as an in situ sensor to monitor the deposition rate of the solid residue and the property changes in liquid during thermal degradation experiments of lubricants. Representative signal profiles (shown in Fig. 7) are extracted to demonstrate the acquisition of pertinent parameters from QCM signals utilizing the approaches presented in Sections 4.1 and 4.2. The temperature of the lubricant increased from the room temperature (around 25 °C) to slightly higher than the set point (220 °C); the system then stabilized at the desired temperature. The resonator ceased to vibrate in the initial heating period until the temperature reached a value of approximately 150 °C. This was attributed to the high viscosity of the lubricant over the lower temperature range [15]. Sensor signals during the initial temperature rise (Phase A) and the isothermal stage (Phase B) were selected for discussion since the features (temperature

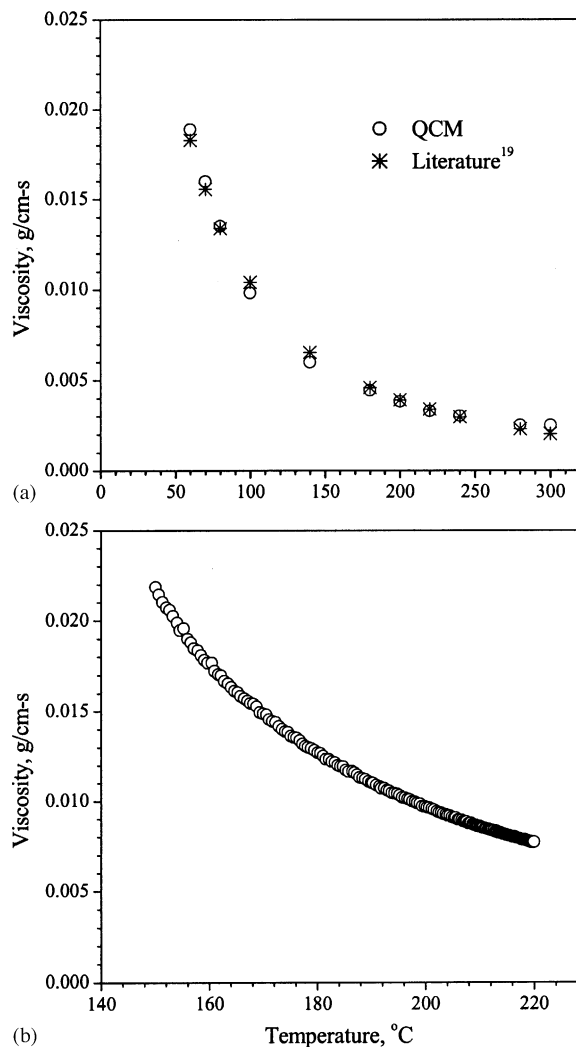


Fig. 6. Temperature dependence of viscosity values for (a) heptadecane and (b) lubricant EM measured using QCM.

effect and property changes) shown in Phases A and B are significantly different. In following section, the two stages will be discussed separately.

##### 4.3.1. Phase A: initial temperature rise period

In Phase A, the measured QCM frequency (Fig. 7b) and damping voltage (Fig. 7c) closely follow the temperature profile (Fig. 7a) since the frequency of quartz and the viscosity of the lubricant are extremely sensitive to small changes in temperature. The frequency shift in Phase A has contributions from the temperature effect and viscous damping, as well as the mass accumulated on the electrode surfaces. To calculate the mass deposited on the electrode surface from the QCM theory (Eq. (2)), the frequency shifts caused by temperature changes,  $\Delta F_T$ , and viscosity changes,  $\Delta F_\eta$ , must be determined first.

The frequency shifts resulting from the temperature effect,  $\Delta F_T$ , are calculated based on Eq. (5). The temperature coefficients  $a_0$ – $a_3$  are obtained from equations listed in Fig. 4 since

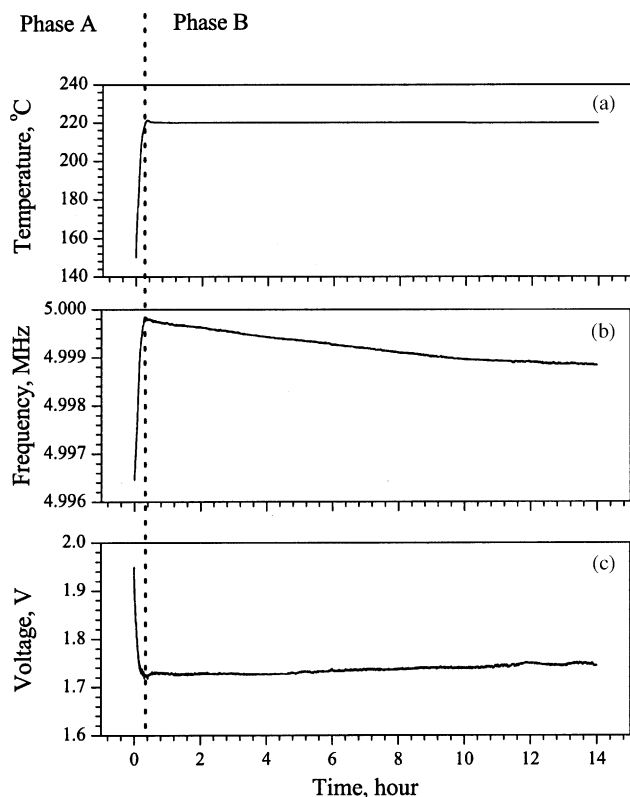


Fig. 7. Time-dependent temperature (a) and QCM responses (frequency (b) and damping voltage (c)) recorded during thermal degradation of lubricant EM. Dashed line separates the two phases: Phase A represents the initial temperature rise; Phase B represents isothermal stage (220 °C).

the temperature of liquid increased continuously at rates that changed gradually. The rates of temperature rise are calculated from the time dependent temperature data (Fig. 7a). The derived time dependent frequency shift,  $\Delta F_T$ , is shown in Fig. 8. In the plots shown in this section, zero on the time axis is defined as the moment when the crystal started vibrat-

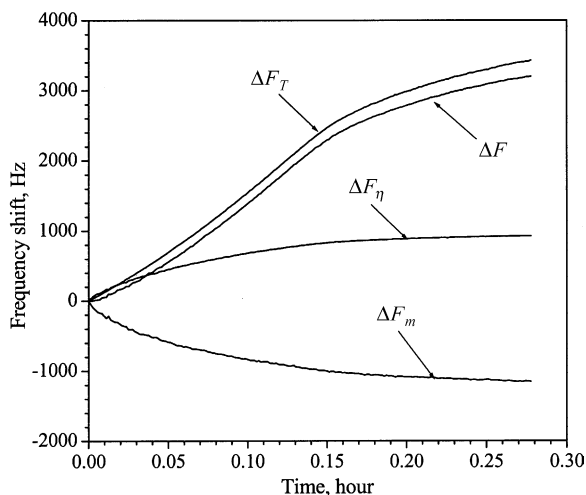


Fig. 8. Total frequency shift ( $\Delta F$ ) and contributions from mass load ( $\Delta F_m$ ) liquid load ( $\Delta F_\eta$ ) and temperature effect ( $\Delta F_T$ ) during the initial temperature rise (Phase A in Fig. 7).

ing in the heated lubricant. It should be pointed out that all of the frequency shifts ( $\Delta F$ ,  $\Delta F_T$ ,  $\Delta F_\eta$ ,  $\Delta F_m$ ) presented in Fig. 8 are the differences between the relative frequencies at time  $t$  and time zero.

The liquid properties, here indicating the product of density and viscosity, change significantly over Phase A. These property variations further affects the frequency shift contribution,  $\Delta F_\eta$ . The density–viscosity products are obtained from the measured damping voltage values (Fig. 7c) using the calibration curve presented in Eq. (10). The values of  $\Delta F_\eta$  are calculated from the density–viscosity products of the liquid based on Eq. (3). The derived time dependent frequency shift,  $\Delta F_\eta$ , is shown in Fig. 8.

The frequency shift,  $\Delta F_m$ , caused by mass deposited on the electrode surfaces was obtained by subtracting  $\Delta F_T$  and  $\Delta F_\eta$  from the total frequency shift  $\Delta F$ . The time dependent values of  $\Delta F$  and  $\Delta F_m$  are also presented in Fig. 8. One of the most important parameters we are interested in during lubricant thermal degradation is the solid residual deposition rate. The following relationship between the rate of mass deposition and the frequency shift  $\Delta F_m$  can be derived from Eq. (2):

$$\frac{d(\Delta m)}{dt} = - \left( \frac{1}{C_m} \right) \left( \frac{d\Delta F_m}{dt} \right) \quad (11)$$

where  $C_m = -(2nF_0^2)/(\mu_q\rho_q)^{1/2}$ . The Origin data analyzing method was utilized to calculate the derivative of  $\Delta F_m$  from the data. The calculated time dependent values of mass deposition rate are shown in Fig. 9. It is seen that there is rapid solid residual deposition in the first few minutes; the rate of solid residual deposition decreases with heating time. The results from the gel permeation chromatography analysis indicate that the mass accumulation in the initial heating stage was mainly caused by the adsorption of pentaerythritol tetrapelargonate [27]. The deposits from generated high molecular weight oxy-polymeric compounds should occur in the further thermal degradation of pentaery-

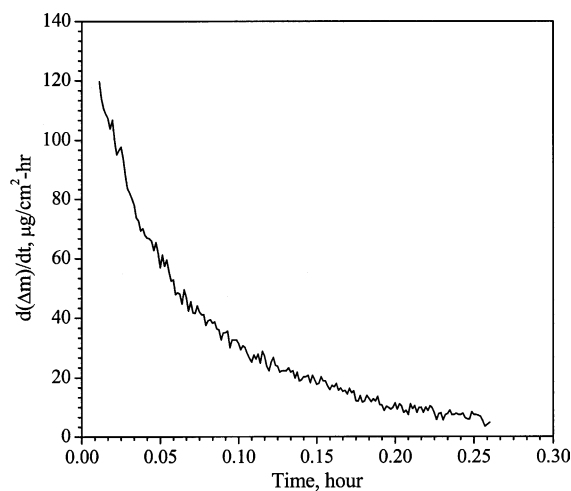


Fig. 9. Variation of solid residual deposition rate of EM during the initial temperature rise (Phase A in Fig. 7).

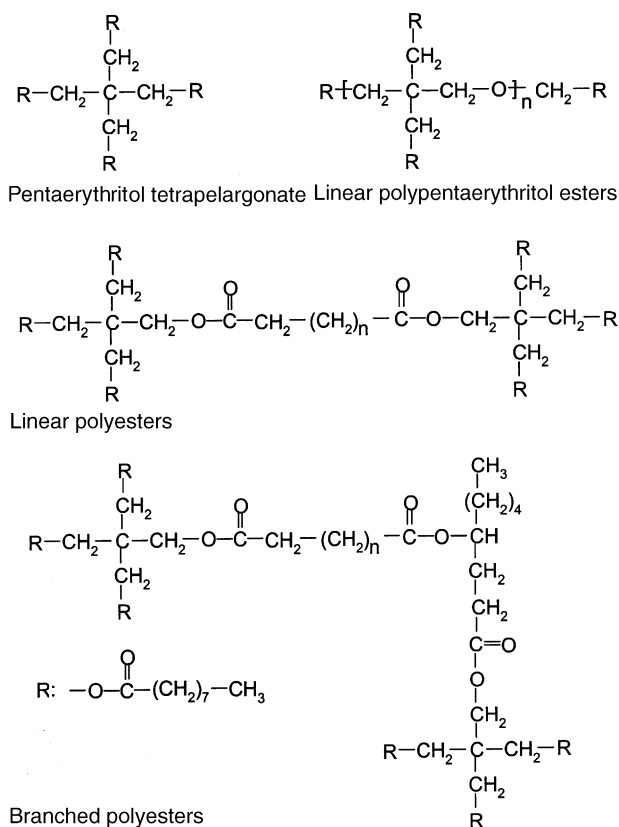


Fig. 10. Structures of pentaerythritol tetrapelargonate (EM) and the major degraded product of oxy-polymeric compounds.

thritol tetrapelargonate. Some of the most probable degraded products include: dipentaerythritol ester, different linear and branched polypentaerythritol esters in addition to different linear and branched polyesters [28,29]. The structures of pentaerythritol tetrapelargonate and samples of polyesters and polypentaerythritol ester are shown in Fig. 10.

#### 4.3.2. Phase B: isothermal period

For the constant-temperature degradation period (Phase B), the total frequency shift was caused only by the viscous damping and mass deposition. To emphasize the features in constant-temperature period, we define: (1) the zero point on the time axis to represent the moment that the liquid temperature becomes stable at 220 °C; (2) the shifts of each defined frequency ( $\Delta F$ ,  $\Delta F_\eta$ ,  $\Delta F_m$ ) are the differences between the relative frequencies at time  $t$  and time zero. The values of  $\Delta F_\eta$  are obtained based on the Eq. (10) from the data represented in Fig. 7 (Phase B). The calculated time dependent values of  $\Delta F$ ,  $\Delta F_\eta$  and  $\Delta F_m$  are shown in Fig. 11. It is obvious that the total frequency shift mainly results from the solid residual deposition. Therefore, the total frequency shift can be used as a quick indicator for evaluating the mass deposition process in the constant temperature conditions over the duration of the current experiment.

Two of the most important parameters, the mass deposition rate and viscosity–density product that characterize the

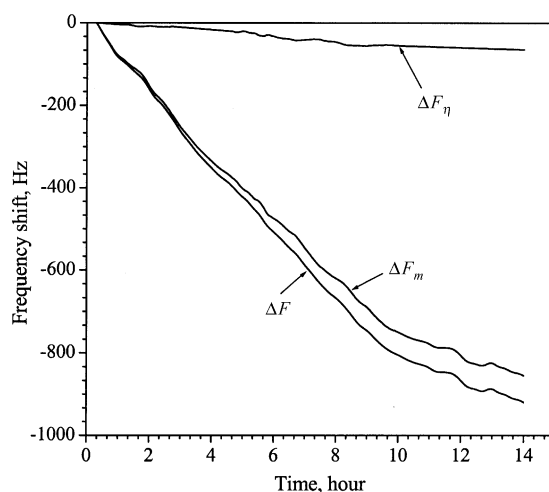


Fig. 11. Frequency shift of EM degradation under isothermal conditions (220 °C, Phase B in Fig. 7).

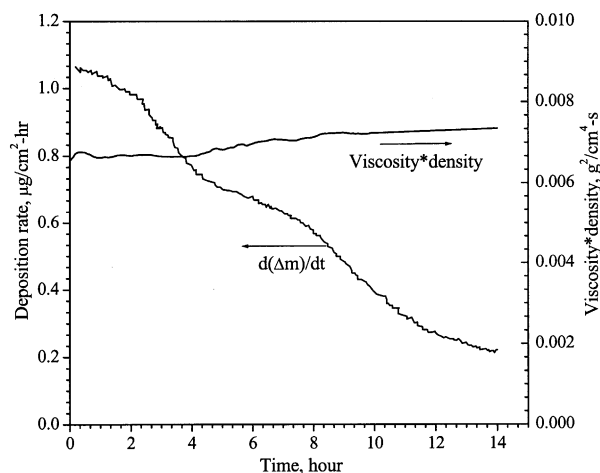


Fig. 12. Plots of solid residual deposition rate and viscosity–density product versus heating time of EM in constant-temperature stage (Phase B in Fig. 7).

lubricant thermal degradation behavior, are shown in Fig. 12. The data indicate that the mass deposition rate decreases with the heating time within the 14 h heating duration. The liquid properties remain relatively constant in the early isothermal period followed by a gradual increase after approximately 4 h of heating at 220 °C.

## 5. Conclusions

The QCM was successfully extended to use in highly viscous liquids at elevated temperatures upwards of 220 °C. A modeling method of temperature compensation was proposed for calculating the temperature effects on resonant frequency for the processes in which the temperature changes continuously. It is revealed that the frequency shift resulting from the temperature change is also the function of the rate of temperature rise in the case of continuous temperature

changes. The accurate determination of temperature dependence of viscosity is evidence of the QCM's potential as an in situ viscosity sensor at elevated temperature conditions. The simultaneous measurement of time dependent frequency shift and damping voltage change allows in situ monitoring of the mass deposition rate and the liquid property changes using the QCM. The solid residual deposition rate and property changes of the pentaerythritol tetrapelargonate based lubricant EM were successfully determined. Our group has demonstrated the capability of the QCM as an in situ sensor in extreme environments such as high pressure [30], viscous fluids [29,31] and liquid systems [32]. This paper further demonstrates the utilization to quantitatively evaluate the thermal degradation behavior of viscous materials at elevated temperatures.

### Acknowledgments

This material is based upon work supported by the National Textile Center (Projects #C01-S08 and #C01-NS08). We are grateful to Dr. Thomas W. Theyson (Goulston Technologies) and Dr. Paul D. Seemuth (Invista) for helpful technical discussions and samples. We acknowledge undergraduate student Richard H. Peak (Louisiana State University) for his assistance with laboratory experiments. Support for undergraduate researchers were provided by NSF Green Processing REU Program (EEC-9912339).

### References

- [1] M.D. Ward, D.A. Buttry, *Science* 249 (4972) (1990) 1000.
- [2] C.K. O'Sullivan, G.G. Guilbault, *Biosens. Bioelectron.* 14 (8–9) (1999) 663.
- [3] G. Sauerbrey, *Zeitschrift fuer Physik* 155 (1959) 206.
- [4] T. Numura, M. Okuhara, *Anal. Chim. Acta* 142 (1982) 281.
- [5] H. Muramatsu, *Anal. Chem.* 60 (1988) 2142.
- [6] S.J. Martin, V.E. Granstaff, G.C. Frye, *Anal. Chem.* 63 (1991) 2272.
- [7] D.A. Buttry, M.D. Ward, *Chem. Rev.* 92 (6) (1992) 1355.
- [8] V. Tsionsky, L. Daikhin, M. Urbakh, E. Gileadi, *Langmuir* 11 (1995) 674.
- [9] V.N. Bakunin, O.P. Parenago, *Synth. Lubr.* 9 (1992) 127.
- [10] S.I. Tseregounis, J.A. Spearot, D.J. Kite, *Ind. Eng. Chem. Res.* 26 (1987) 886.
- [11] S. Zabarnick, S.D. Whitacre, *J. Eng. Gas Turbines Power* 120 (1998) 519.
- [12] C. Lu, A.W. Czanderna, *Application of Piezoelectric Quartz Crystal Microbalance*, Elsevier, New York, 1984.
- [13] Z.Y. Lin, C.M. Joseph, I.S. and, M.D. Ward, *Anal. Chem.* 65 (1993) 1546.
- [14] K.K. Kanasawa, J.G. Gordon, *Anal. Chem.* 57 (1985) 1770.
- [15] M. Yang, M. Thompson, *Anal. Chem.* 65 (1993) 1158.
- [16] V.E. Bottom, *Introduction to Quartz Crystal Unit Design*, Van Nostrand Reinhold, New York, 1982.
- [17] V.M. Mecea, J.O. Carlsson, P. Sessler, M. Bartan, *Vacuum* 46 (1995) 691.
- [18] M.E. Frerking, *Crystal Oscillator Design and Temperature Compensation*, Van Nostrand Reinhold, New York, 1978.
- [19] R. Bechmann, *Proc. IRE* 48 (8) (1960) 1494.
- [20] K.O. Wessendorf, *IEEE International Frequency Control Symposium*, 1993, p. 711.
- [21] B.E. Poling, J.M. Prausnitz, J.P. O'Connell, *The Properties of Gases and Liquids*, McGraw-Hill, New York, 2001.
- [22] R. Bechmann, *Proc. IRE* 44 (11) (1956) 1600.
- [23] A.R. Chi, *Proceedings of 10th Annual Symposium Frequency Control*, 1956, p. 46.
- [24] [www.gequartz.com/en/cruproperties.htm](http://www.gequartz.com/en/cruproperties.htm), 2004.
- [25] T.J. O'Hern, W.M. Trott, S.J. Martin, E.A. Klavetter, *AIAA Paper*, AIAA-93-0363, the Aerospace Science Meeting, Reno, NV, 1993.
- [26] S.K. Naidu, E.E. LKlaus, J.L. Duda, *Ind. Eng. Chem. Prod. Res. Dev.* 25 (1986) 596.
- [27] P. Mousavi, Ph.D. Thesis, NC State University, 2004.
- [28] B. Koch, E. Jantzen, *J. Synth. Lubr.* 4 (1987) 321.
- [29] P. Mousavi, D. Wang, C.S. Grant, P.J. Hauser, W. Oxenham, *Ind. Eng. Chem. Res.* 44 (15) (2005) 5455.
- [30] Y. Wu, P.J. Akoto-Ampaw, M. Elbaccouch, M.L. Hurrey, S.L. Wallen, C.S. Grant, *Langmuir* 20 (9) (2004) 3665.
- [31] D. Wang, P. Mousavi, P.J. Hauser, W. Oxenham, C.S. Grant, *Ind. Eng. Chem. Res.* 43 (21) (2004) 6638.
- [32] Y. Hussain, J. Krim, C.S. Grant, *Colloids Surf. A: Physicochem. Eng. Aspects* 262 (1–3) (2005) 81.